Available online at www.sciencedirect.com
SCIENCE DIRECT
ELSEVIER
International Journal of Mass Spectrometry 254 (2006) 189–196
International Journal of Mass Spectrometry
www.elsevier.com/locate/ijms

C–H activation in reactions of protonated hydrogen peroxide with propane Remarkable regioselectivity for hydride abstraction and mechanism for acid catalyzed hydrogen exchange

Christian Adlhart, Einar Uggerud *

Department of Chemistry, University of Oslo, P.O. Box 1033, Blindern, N-0315 Oslo, Norway

Received 7 February 2006; received in revised form 24 May 2006; accepted 24 May 2006
Available online 27 June 2006

Abstract

Reactions between deuterium labelled alkanes and H_2OOH^+ have been investigated by conducting gas phase reactions within the cell of an FT-ICR mass spectrometer. Propane is exceptional in giving off a hydride (deuteride) thereby producing the propyl cation and two water molecules, as well as demonstrating high activity for proton induced H/D exchange. The detailed mechanistic scenario has been modelled using accurate quantum chemical methods (MP2 and G3). The calculations show that hydrogen exchange takes place via a synchronous flip–flop mechanism. Results of reactions with partially deuteriated propanes demonstrate quite exceptional regioselectivity for hydride abstraction in favour of the secondary positions (2-H) compared to the primary (1-H). This observation is understood on the basis of transition state theory.

Keywords: Mass spectrometry; Carbocations; Reaction mechanism; Proton transfer; Hydride abstraction; Alkanium ions; Quantum chemistry

1. Introduction

Controlled activation of bonds between carbon and hydrogen is prerequisite for all types of functionalisation of alkanes, including oxidation. For this reason C–H bond activation continues to be a subject of great interest both in industry and academia. A lot of effort has been put into transition metal research [1–3]. However, for direct and selective oxidation of alkanes, for example, conversion of methane to methanol, no efficient transition metal catalyst has yet been found. Alternative strategies for direct oxidation should therefore also be investigated.

Recently, it was demonstrated experimentally that free molecules of protonated hydrogen peroxide are powerful oxidants since they react with all alkanes except methane [4]. Earlier work had shown that butane is oxidized to butanol in super acidic solutions of hydrogen peroxide [5–7]. The key step is hydride abstraction from the alkane to the ion [4,8]

$$RH + H_2OOH^+ \rightarrow R^+ + 2H_2O \quad (1)$$

Protonated hydrogen peroxide is member of a larger family of potential oxidants, which may be considered as ligated hydroxyl cations, L-OH^+ (L = H_2O, NH_3, *p*-methyl-pyridine). It has been shown, by experiment and theoretical modelling, that the oxidation power of such cations depends on the Lewis basicity of L; the better electron donor, the poorer oxidant [9].

In addition to being potential two-electron oxidants, these species are also potential proton donors. It is well known that C–H activation is the result when an alkane is protonated. Any compound of sufficient acidity may transfer a proton to an alkane thereby giving rise to an alkanium ion, $C_nH_{2n+3}^+$. This was observed independently by Olah et al. [10,11] and Hogeveen and Bickel [12] from studies of super acid solutions in the late 1960s. As a matter of fact, alkanium ions were well known from mass spectrometric studies already in the early 1950s [13,14]. This and the above examples show that the gas phase is an ideal medium for studying elusive ionic species and their reactivity. An interesting point in the present context is the particular molecular and electronic structure of alkanium ions. Since all available valences of the carbon atoms of alkanes are occupied by an atom, adding a proton will break the classical structure, and the result is a hypervalent species with half bonds between carbon and hydrogen and sometimes also between two car-

* Corresponding author. Tel.: +47 22 85 55 37; fax: +47 22 85 54 41.
E-mail address: einar.uggerud@kjemi.uio.no (E. Uggerud).

1387-3806/$ – see front matter © 2006 Elsevier B.V. All rights reserved.
doi:10.1016/j.ijms.2006.05.018

bon atoms—in other words, bond activation has been achieved [15].

From previous work we were able to identify the primary mechanism of the reaction between protonated hydrogen peroxide and alkanes [4]. However, important mechanistic questions remain unanswered. Propane and larger alkanes have hydrogen atoms in structurally non-equivalent positions. It would be extremely interesting to see if hydride abstraction demonstrates any regioselectivity, and in case it does, reveal the factors that determine reactivity. Moreover, larger alkanes have higher proton affinities (PA) than small alkanes. If the alkane has a sufficiently high PA, we could expect C–H activation through proton transfer. From experiments with propane in HF/SbF_5 super acid, it has been demonstrated that H/D exchange takes place [16]. To answer these pertinent questions, we decided to investigate reactions between protonated hydrogen peroxide and suitably deuterium labelled alkanes. In addition, we performed *ab initio* quantum chemical calculations to model the reaction mechanisms under investigation.

2. Experimental and computational methods

2.1. Experiment

$HOOH_2^+$ was produced from the mixed urea and hydrogen peroxide formulation (synthesized and prepared in the laboratory [17]), in an external ion source using chemical ionisation with methane. To avoid decomposition of the formulated hydrogen peroxide in the gas/liquid sample introduction system, a direct inlet probe (DIP) equipped with a glass container rather than the normal aluminium container was used. The DIP was kept at $t = 0\,^{\circ}C$. The ions formed in the source were transferred to the cell of an FT-ICR mass spectrometer, a Bruker 4.7 T Bio Apex (Billerica, MA, USA). Substrates, ethane-1,1,1-d_3 (99 atom%), propane-2,2-d_2 (99 atom%), and propane-1,1,1,3,3,3-d_6 (98 atom%, all Icon Isotopes, USA) were dispensed into the FT-ICR cell through a leak valve ($p = 2.0 \times 10^{-9}$ mbar to 1.5×10^{-7} mbar). Ion isolation and all subsequent isolation steps were performed using a computer controlled ion-ejection protocol, which combines single frequency ion-ejection pulses with frequency sweeps. Briefly, all ions except the chosen reactant ion were ejected from the cell by this procedure. The remaining population of H_2OOH^+ ions was cooled to ambient temperature upon introduction of a short pulse of argon (peak-pressure around, $p = 1 \times 10^{-6}$ mbar). The reactant ions were then again isolated by single optimised frequency shots that removed ions formed during the cooling period of 2 s. After this process the ions were allowed to react freely with the substrate for a time delay of 4 s before a mass spectrum was recorded. To account for minor contributions from light ions ($m/z \leq 14$) – neither observable nor ejectable in the FT-ICR – control experiments were run in which also H_2OOH^+ was ejected from the cell. A background spectrum obtained in this manner was then subtracted from the original spectrum. The substrate pressure was determined via the use of a cold cathode ion gauge that was calibrated against the reaction of $NH_3^{\bullet+}$ (generated externally by EI) plus NH_3, $k_r = 2.2 \times 10^{-9}$ cm^3 mol^{-1} s^{-1} [18,19].

2.2. Computations

In order to estimate the energetics of potential reaction channels a series of *ab initio* calculations were conducted employing the Gaussian 03 suite of programs [20]. Initially, MP2 calculations were done with the 6-31G(d) basis sets. All stationary points were subject to complete geometry optimisation, including a check for the correct number of negative Hessian eigenvalues and imaginary frequencies. To obtain more accurate estimates for the energies, G3 theory calculations were used. G3 is a composite technique, which involves several geometry optimisations and energy evaluations at the HF, MP2 (full), MP4 levels as well as coupled cluster calculations. For a further description see reference [21]. As a modification, we froze the MP2/6-31G(d) geometries throughout the G3 procedure, as described previously [9,22]. We use $G3_m$ as notation for the modified G3 scheme. All calculations relate to the singlet electronic state throughout, as the corresponding triplet state energies are known to be sufficiently high not to be of relevance to the present reactions [23,24].

Statistical rate coefficients for the hydride abstraction reactions and the flip–flop proton exchange [25] were calculated with a modified RRKM program originally from Sture Nordholm, Göteborg, employing spectroscopic constants (moments of inertia and harmonic vibrational frequencies) from the $G3_m$ calculations. To account for tunnelling probabilities, the potential energy surface at the transition state was approximated by a parabolic fit based on the imaginary frequency.

3. Results and discussion

3.1. Hydride abstraction

The reaction of H_2OOH^+ with C_2H_6 is slow ($k = 5 \times 10^{-11}$ cm^3 molecule^{-1} s^{-1}) [4]. The corresponding reaction with ethane-1,1,1-d_3 appears to be equally slow or even slower, and a rather poor signal-to-noise ratio did unfortunately not allow us to determine rate coefficients, regioselectivity or isotope effects with confidence. On this basis, the rest of the discussion will be limited to the results for the isotopically labelled propanes.

In the reactions with deuterated propane ($k = 4 \times 10^{-10}$ cm^3 molecule^{-1} s^{-1}) [4] we observed the expected hydride abstraction (approximately 92%)

$$C_3H_8 + H_2OOH^+ \rightarrow C_3H_7^+ + 2H_2O \quad (2)$$

In addition the experiments displayed results due to two additional reaction channels:

$$C_3H_8 + H_2OOH^+ \rightarrow C_3H_6 + H_2O + H_3O^+ \quad (3)$$

and (approximately 8%)

$$C_3H_7\mathbf{H} + [HOOH]H^+ \rightarrow C_3H_8 + [HOOH]\mathbf{H}^+ \quad (4)$$

Table 1
Temperature dependence of the various relative reaction rates obtained using $G3_m$ energies and the Arrhenius equation

	Temperature (K)		
	298	388	530
k_1/k_2	0.066	0.123	0.216
k_{1H}/k_{1D}	1.68	1.49	1.34
k_{2H}/k_{2D}	1.81	1.58	1.40

Reaction (3) was reported in the earlier study and the product hydroxonium ion is formed via proton transfer within the intermediate $[C_3H_7\cdots H_2O]^+$. The hydrogen exchange reaction (4) has not yet been reported, and it represents a very intriguing observation, since it shows that the C–H activation of the propane is taking place. This will be discussed later on. The ratio for Reaction (3) cannot be assigned unambiguously, since formation of H_3O^+ may also be due to proton transfer from H_2OOH^+ to background water [4]. The latter, as well as the related identity S_N2 reaction of H_2OOH^+ and H_2O, have recently been studied theoretically by *ab initio* molecular dynamics simulations [26].

For both labelled propanes, two product peaks were observed, which means that H_2OOH^+ abstracts a hydride from either the 1- or the 2-position. The analysis of reaction rates can be done in two different ways. The best would be to compare the absolute rates for abstraction of hydride in either the 1- or the 2-position for the two isotopomers, thereby directly providing the ratios of interest, namely k_1/k_2, as well as the isotope effects k_{1H}/k_{1D}, and k_{2H}/k_{2D}. Regrettably, the absolute error of FT-ICR gas phase ion molecule rates is too high (in unfavourable cases up to ±40%), not allowing determination of normal isotope effects. There is little to do in order to circumvent this situation, since the uncertainty comes from unreliable determination of the absolute pressure using an ion gauge. The alternative method – which we have been left with in the present case – is to take advantage of the high accuracy of peak area determination, and make the estimates based on the relative peak areas obtained in the separate measurements with the two complementary isotopomers. The obvious drawback of this approach is that we are left with an under-determined set of equations, in the sense that we want to estimate three ratios k_1/k_2, k_{1H}/k_{1D}, and k_{2H}/k_{2D}, but have only access to the experimental numbers k_{1H}/k_{2D} and k_{2H}/k_{1D}. For this reason we had to make one simplification, namely setting the isotope effects for the 1- and the 2-positions to be equal. This approximation is justified on the basis of the quantum chemical calculations that showed the theoretical isotope effects to be identical within ±4% (Table 1, *vide infra*) (Fig. 1).

Introducing this approximation we obtain the following results:

$$\frac{k_1}{k_2} = 0.123 \pm 0.012,$$

and

$$\frac{k_H}{k_D} = 1.24 \pm 0.13.$$

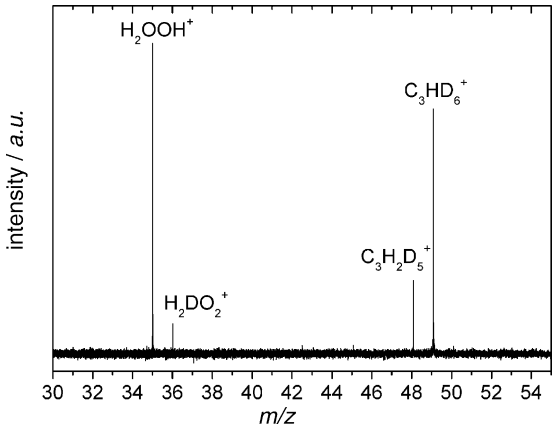

Fig. 1. Excerpt of the difference mass spectrum obtained after 4 s for the reaction between the $CD_3CH_2CD_3$ and $H_3O_2^+$.

The uncertainty estimate is based on systematic errors from three sources: the limitation in the signal to noise ratio, inaccuracy in product ion peaks arising from reactions of energetic ions with $m/z \leq 14$ (<10%), and errors introduced by the side reactions (<10%).

The hydride abstraction reaction is exothermic by 312 kJ mol^{-1}, *vide infra*. On the basis of this considerable figure alone, one might anticipate hydride abstraction to be completely indiscriminating with regard to which hydrogen atom is removed. It is therefore highly remarkable that we observe a regioselectivity of this magnitude in favour of the central methylene group. Theoretical calculations may provide the explanation.

Fig. 2 shows the $G3_m$ transition structure energies and the embedded MP2/6-31G(d) geometries of the transition structures for hydride abstraction. Since the potential energy barrier for abstraction of a hydride from methane is at +12 kJ mol^{-1} relative to the total potential energy of the reactants, no reaction is observed for this alkane. For ethane the barrier is at −7 kJ mol^{-1} relative to the reactants, which nicely explains the slow rate, observed in this case. For propane there are two barriers, one for attack on one of the hydrogen atoms of the methylene group (2-H) and one for attack on one of the hydrogen atoms of the methyl groups (1-H). Both barriers are below that for ethane, and the barrier for 2-H is the lowest. In order to understand the experimentally observed regioselectivity, the existence of the two barriers as well as the potential energy minimum corresponding to the reactant complex $[C_3H_8\cdots H_2OOH]^+$ (**13**) (Fig. 3) has to be accounted for. Only the existence of a long-lived intermediate that exhibits ergodic behaviour can explain the delicate discrimination in favour of the hydride transfer with the lowest barrier, even though both barriers are well below the total energy of the reactants (*i.e.*, the potential energy has a negative value), and that the energy difference between the related transition structures is only around 6 kJ mol^{-1}. This situation can nicely be put into quantitative terms by applying reaction rate theory. The simplest is the use of the Arrhenius equation. The necessary activation entropies and enthalpies were estimated using relative energies and explicit spectroscopic data for the isotopomers (frequencies and moments of inertia) from the $G3_m$ calculations.

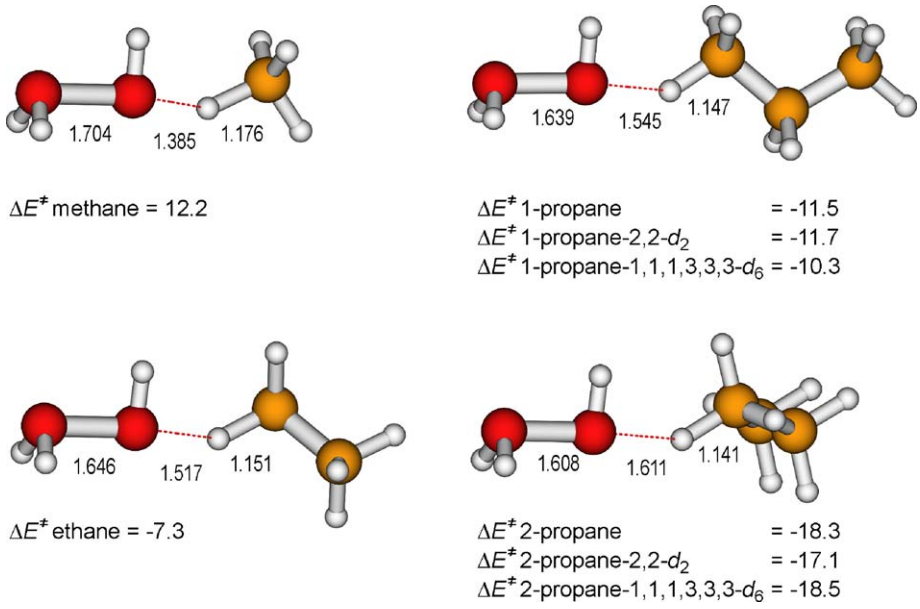

Fig. 2. Transition structures (bond lengths in Å) and corresponding $G3_m$ energies (kJ mol^{-1}) for the hydride abstraction reactions. The energies are relative to the respective separated reactants $RH + H_2OOH^+$.

It can be seen that the experimental ratio k_1/k_2, which describes the regioselectivity, is smaller than the corresponding theoretical figure at room temperature (Table 1). However, one should note that there is an amount of energy not accounted for by this simple approach. By adding the complexation energy of 33.8 kJ mol^{-1} to the reactant complex $[C_3H_8\cdots H_2OOH]^+$ (**13**) distributing it statistically among the degrees of freedom, we obtain an upper limit for the complex temperature of 530 K. The best match with our experimental value is obtained for a complex temperature of 388 K. Any value between 298 K and 530 K is fully acceptable taking the experimental uncertainty as well as the low reaction efficiency of <10% into account. For example, there are ample possibilities for collisional and even radiative cooling (Fig. 4).

An alternative, and *a priori* more accurate, treatment can be obtained using RRKM theory. In Fig. 3 we have displayed the outcome of our calculations, again obtained using the $G3_m$ data. In this case, the theoretical model is also very good. The discrepancy is consistent with inaccuracies in the relative barriers of 1–2 kJ mol^{-1}. In essence, we conclude that the theoretical models give very satisfactory descriptions of the experimental observations.

3.2. Proton exchange

The observation of the peak due to $H_2O_2D^+$ (Fig. 1) and its variation with time is clear evidence for proton exchange between protonated hydrogen peroxide and propane. As already mentioned, C_3H_8 is not sufficiently basic to be protonated by $H_2O_2H^+$, also evident by the fact that the proton resides within the H_2OOH^+ unit in the addition complex **13**. There is no minimum corresponding to $[C_3H_9\cdots HOOH]^+$ but the relatively small

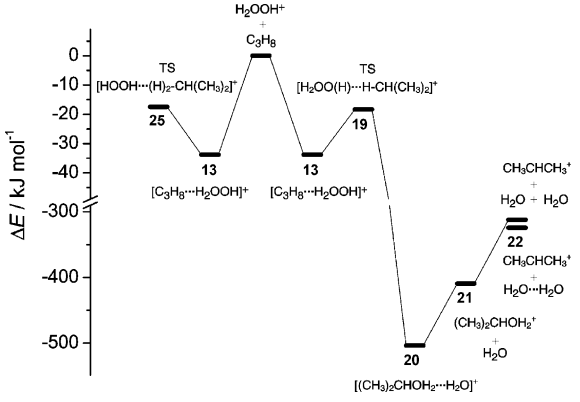

Fig. 3. Potential energy diagram for the reaction of protonated hydrogen peroxide with propane, obtained by the $G3_m$ method. Both the proton exchange reaction (synchronous flip–flop mechanism) and the hydride abstraction from the 2-position are shown. The numbers refer to the structures as provided in the supplementary material.

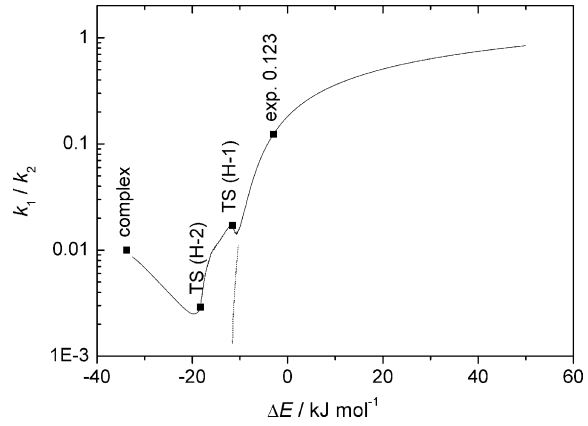

Fig. 4. Theoretical relative rates (k_{H1}/k_{H2}) obtained from RRKM calculations; solid line: RRKM rates including tunnelling; dashed line: RRKM rates without tunnelling. Energies are relative to the free reactants. The experimental ratio (0.123 ± 0.012) corresponds to 30.8 kJ mol^{-1} internal energy.

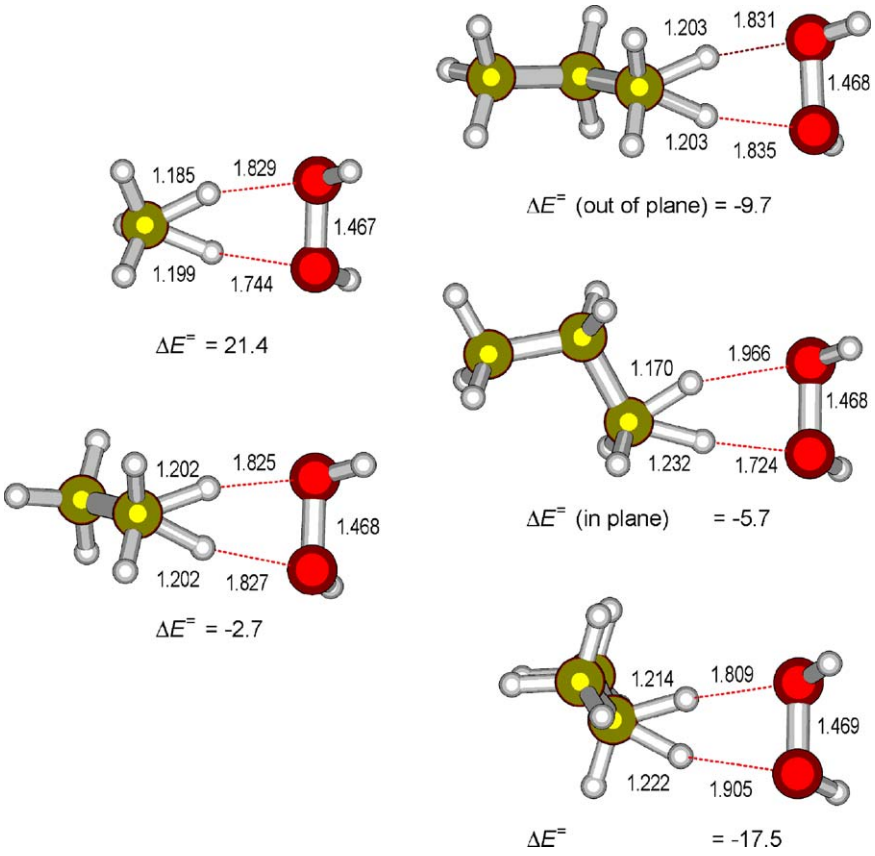

Fig. 5. Transition structures (bond lengths in Å) and corresponding $G3_m$ energies (kJ mol^{-1}) for the proton exchange reaction (synchronous flip–flop mechanism). The energies are relative to the respective separated reactants $RH + H_2OOH^+$.

difference in proton affinity between propane and hydrogen peroxide of 49 [51] kJ mol^{-1} (experimental value [G3 value]) [27,9] could allow for an exchange reaction within the complex. In order to investigate the energetic, mechanistic, and structural features of the exchange, we performed further quantum chemical calculations. We were able to locate the transition structures displayed in Fig. 5, not only for propane but also for methane and ethane. While the potential energy minima corresponding to complexes between protonated hydrogen peroxide and the alkanes are of the type $[C_nH_{2n+2}\cdots H_2OOH]^+$, the transition structures represent the complementary complexes between the hypervalent alkanium ions and hydrogen peroxide, $[C_nH_{2n+3}\cdots HOOH]^+$.

Table 2 gives the relative energies and entropies for the reaction of H_2OOH^+ with methane, ethane, propane (1-H), and propane (2-H) in analogy to the potential energy diagram for propane (2-H) (Fig. 3). It is fascinating how closely the transition structure energies for proton exchange and hydride abstraction follow each other (Figs. 2 and 5; Table 2); methane does not allow for any of the reactions, ethane barely opens up for both, while hydride abstraction and proton exchange are evident for propane. As a matter of fact, there is perfect linear correlation between the two sets of transition structure energies, and each shows good linear correlation with the substituent *a*-values [28] for methyl, ethyl, and isopropyl. It is also illustrative that the three transition structures for each propane reaction correspond to one of the three tautomers of protonated propane: the 2-protonated, the in-plane 1-protonated, and the out-of-plane 1-protonated [29]. Already in 1938 it was suggested that the three hydrogen nuclei of H_3^+ (protonated dihydrogen) form the corners of an equilateral triangle [30]. This has later been confirmed [31,32]. Although CH_5^+ and $C_2H_7^+$ are quite stable structures [15,33], larger alkanium ions appear to be fragile molecular entities. This includes the three isomers of $C_3H_9^+$ that are all highly unstable in their own right, since they are known to undergo easy dehydrogenation or demethanation [29,34]. However, during the extremely short lifetime of the transition structure no decomposition of the propane molecule occurs. This is manifested in our experimental observation that loss of CH_4 remains unobserved. This is also consistent with the finding that propane does not undergo any skeletal rearrangement in HF/SbF_5 solution, although extensive H/D exchange occurs [16].

The reaction coordinate is best characterized as a synchronous motion of the incoming and an outgoing proton (synchronous flip–flop mechanism, Fig. 5). In terms of the transient propanium molecule this corresponds to the asymmetric combination of the corresponding C–H stretches. The hydrogen peroxide part acts as bidendate base by accepting the incoming proton at the other oxygen site than the site of the departing proton. This arrangement is obviously stereo-electronically very favourable. Based on quantum chemical model calculations a completely analogous mechanism has been suggested for the H/D exchange observed for propane over a zeolite catalyst (H–ZSM-5) [35]. Two separate oxygen sites of the partially protonated zeolite are

Table 2
Results from the quantum chemical calculations

		MP2/6-31G(d), ΔE (kJ mol^{-1})	MP2/6-31G(d), ΔS (J mol^{-1} K^{-1})	MP2/6-31G(d), ΔG° (kJ mol^{-1})	$G3_m$, ΔE (kJ mol^{-1})
$[H_2OOH\cdots CH_4]^+$	**1**	−15.3	−99	14.4	−18.9
TS $[H_2OO(H)\cdots H\text{-}CH_3]^+$	**2**	23.8	−118	57.3	12.2
$[CH_3OH_2\cdots H_2O]^+$	**3**	−429.6	−131	−392.8	−433.8
$CH_3OH_2^+$	**4**	−301.5	−10	−297.7	−323.4
CH_3^+[a]	**5**	−27.9	52	−36.6	−67.9
CH_3^+[b]	**5**	−7.0	137	−38.8	−55.5
TS $[HOOH\cdots(H)_2\text{-}CH_3]^+$	**6**	33.1	−136	69.5	21.4
$[H_2OOH\cdots C_2H_6]^+$	**7**	−21.3	−101	9.9	−26.0
TS $[H_2OO(H)\cdots H\text{-}CH_2CH_3]^+$	**8**	2.5	−124	39.0	−7.3
$[CH_3CH_2OH_2\cdots H_2O]^+$	**9**	−468.4	−134	−429.1	−473.8
$CH_3CH_2OH_2^+$	**10**	−348.5	−14	−342.5	−371.6
$C_2H_5^+$[a]	**11**	−199.1	49	−207.8	−244.8
$C_2H_5^+$[b]	**11**	−178.2	164	−210.0	−232.5
TS $[HOOH\cdots(H)_2\text{-}CH_2CH_3]^+$	**12**	11.7	−142	51.6	−2.7
$[H_2OOH\cdots C_3H_8]^+$	**13**	−27.8	−109	5.8	−33.8
$[H_2OOH\cdots CH_3CD_2CH_3]^+$	**13**-d_2	−27.9	−108.7	5.7	−33.9
$[H_2OOH\cdots CD_3CH_2CD_3]^+$	**13**-d_6	−27.9	−109.0	6.0	−33.9
TS $[H_2OO(H)\cdots H\text{-}CH_2CH_2CH_3]^+$	**14**	−1.7	−114	32.4	−11.5
TS $[H_2OO(H)\cdots H\text{-}CH_2CD_2CH_3]^+$	**14**-d_2	−1.8	−113.9	32.2	−11.7
TS $[H_2OO(H)\cdots D\text{-}CD_2CH_2CD_3]^+$	**14**-d_6	−0.5	−114.3	33.8	−10.3
$[CH_3CH_2CH_2OH_2\cdots H_2O]^+$	**15**	−472.1	−126	−434.2	−478.4
$CH_3CH_2CH_2OH_2^+$	**16**	−354.1	−6	−349.6	−378.0
TS $[HOOH\cdots(H)_2\text{-}CH_2CH_2CH_3]^+$ (out of plane)	**17**	4.7	−131	41.8	−9.7
TS $[HOOH\cdots(H)_2\text{-}CH_2CH_2CH_3]^+$ (in plane)	**18**	6.3	−143	46.5	−5.7
TS $[H_2OO(H)\cdots H\text{-}CH(CH_3)_2]^+$	**19**	−9.5	−123	26.9	−18.3
TS $[H_2OO(H)\cdots D\text{-}CD(CH_3)_2]^+$	**19**-d_2	−8.3	−123.4	28.4	−17.1
TS $[H_2OO(H)\cdots H\text{-}CH(CD_3)_2]^+$	**19**-d_6	−9.7	−123.2	26.9	−18.5
$[(CH_3)_2CHOH_2\cdots H_2O]^+$	**20**	−499.0	−136	−458.6	−503.8
$(CH_3)_2CHOH_2^+$	**21**	−386.4	−11	−380.7	−409.4
$CH_3CHCH_3^+$[a]	**22**	−279.2	68	−291.8	−324.2
$CH_3CHCH_3^+$[b]	**22**	−258.2	153	−294.0	−311.8
cyclo-$C_3H_7^+$[b]	**23**	−231.2	145	−265.8	−276.5
TS 1,2 H-shift $[CH_2(H)CHCH_3]^+$[c]	**24**	−238.0	151	−274.3	−292.3
TS $[HOOH\cdots(H)_2\text{-}CH(CH_3)_2]^+$	**25**	−1.9	−137	37.1	−17.5

[a] The neutral product is a water dimmer.
[b] The neutral products are two water molecules.
[c] Convergence criteria for geometry optimisation were not met, but one imaginary frequency is found for the current structure.

involved in the synchronous exchange. The same mechanism has also been inferred for H/D exchange for propane in super acidic solutions, also this from quantum chemical calculations [34]. In that case the SbF_5 unit acts as a bidendate base by involving two of the fluorine atoms in the synchronous exchange.

3.3. Implications for methane, ethane, propane, and higher alkanes

We have already mentioned the correlation between the transition structure energies for proton exchange and hydride abstraction. The statistical rate analysis reveals an increasing preference for proton exchange for the higher and more basic alkanes (Fig. 6). The upper limit for the available energy in the $[alkane\cdots H_2OOH]^+$ complexes is estimated by adding the complexation energy and the thermal energy of the free reactants to the complex. While the energy is not sufficient for proton exchange in methane (Fig. 6b), proton exchange becomes competitive for the more basic propane, $k_{hydride}/k_{proton} = 4.3$. The basicity as principal driving force for proton exchange reaction is also consistent with the transition structures, where the proton in all cases is located on the alkane rather than on HOOH according to $[C_nH_{2n+3}\cdots HOOH]^+$. The nascent positive charge of the transition structure for the hydride transfer will be influenced in a similar way. Both transition structures therefore depend directly on the capability of R to stabilize the charge – expressed as *a*-values [28] – but to different extent. Propane represents a crossing point between the tendencies for hydride abstraction and proton exchange/transfer, and is unique in the sense that both reactions proceed at similar rates (Fig. 6).

The next higher alkanes – *n*-butane and isobutane – are borderline cases. The proton affinity of isobutane is 678/686 kJ mol^{-1} (experimental value/G3 value) [27,9] above the PA of HOOH, 675/668 kJ mol^{-1}. Larger alkanes will therefore have a tendency towards protonation, and the so-formed alkanium ion will decompose, as discussed above. The two major decomposition reactions of alkanium ions are loss of dihydrogen or loss of methane. This leads us to consider an additional

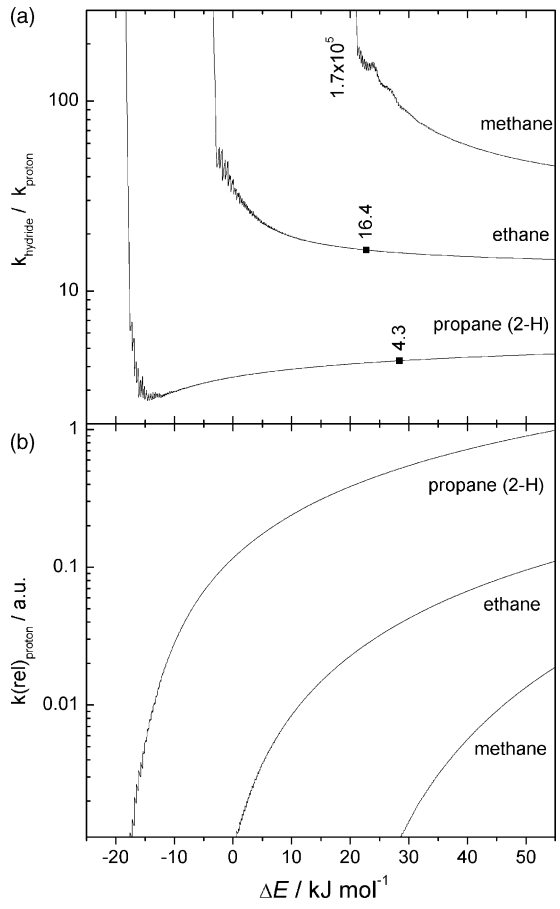

Fig. 6. (a) Theoretical relative rates ($k_{hydride}/k_{proton}$) obtained from RRKM calculations for the hydride abstraction and proton exchange reaction. Tunnelling is included. The estimated upper limits for the relative internal energy for the [alkane···H_2OOH]$^+$ complexes are 18.5 kJ mol^{-1}, 22.7 kJ mol^{-1}, and 28.4 kJ mol^{-1} for methane through propane and $k_{hydride}/k_{proton}$ are 1.7×10^5, 16.4, and 4.3, respectively. (b) Relative rates $k_{(rel)proton}$ for the proton exchange reaction.

mechanism for alkyl cation formation from alkanes larger than propane.

$$C_nH_{2n+2} + H_2OOH^+ \rightarrow C_nH_{2n+1}{}^+ + HOOH + H_2, \quad (5)$$

and

$$C_nH_{2n+2} + H_2OOH^+ \rightarrow C_{n-1}H_{2n-1}{}^+ + HOOH + CH_4. \quad (6)$$

Based on our experiments, we can differentiate between these two mechanisms and we find that loss of methane is not observed in the case of butane. However, we cannot differentiate readily between the formation of $C_nH_{2n+1}{}^+$ through Reaction (5) or through hydride transfer (Reaction (1)). For example, using available thermochemical data [27,36] and combining them with the reaction energy of −372 kJ mol^{-1} for Reaction (1) [4,27], we find that Reaction (5) is 26 kJ mol^{-1} exothermic while Reaction (6) is 6 kJ mol^{-1} endothermic. Whether Reaction (1) or Reaction (5) therefore accounts for the experimentally observed $C_4H_9{}^+$ remains unsettled for the moment. However, in the case of propane, a similar estimate rules out any other mechanism but hydride abstraction.

From an industrial perspective, utilizing propane and hydrogen peroxide to accomplish both oxidative dehydrogenation to produce propene (Reaction (3)) and partial oxidation to produce propanol

$$C_3H_8 + H_2OOH^+ \rightarrow C_3H_7OH_2{}^+ + H_2O \quad (7)$$

are feasible under acidic conditions, as demonstrated above. In the gas phase it becomes difficult to accomplish a full catalytic cycle since the proton affinity of hydrogen peroxide is lower than both that of water, isopropanol, and propene, so proton transfer back from the product to hydrogen peroxide can therefore not be achieved. This fact does of course not rule out the possibility for acidic catalysis in a condensed medium (solution, zeolite, *etc.*).

4. Conclusions

The gas phase reactions between deuterium labelled alkanes and H_2OOH^+ have been investigated and two different C–H activation products have been identified:

(a) alkyl cations due to hydride abstraction;
(b) proton induced hydrogen exchange product.

Both reactions demonstrate strong dependency on the basicity of the alkane and on its capability of stabilizing a positive charge during the hydride transfer.

The detailed mechanistic scenario has been modelled using accurate quantum chemical methods and we found a linear dependency of the transition state energies for hydride transfer and proton exchange. The transition structure for the proton exchange reaction is characterized by a synchronous motion of the incoming and an outgoing proton (synchronous flip–flop mechanism) and the hydrogen peroxide part acts as bidendate base by accepting the incoming proton at the other oxygen site than the site of the departing proton. The same mechanism has been inferred for H/D exchange for propane in super acidic solutions as well as over zeolite catalysts where two separate oxygen sites of the partially protonated zeolite are involved in the synchronous exchange. The transition structures for the proton exchange reactions represent complexes between the hypervalent alkanium ions and hydrogen peroxide, $[C_nH_{2n+3}\cdots HOOH]^+$. For propane, three transition structures were identified, each corresponding to one of the three tautomers of protonated propane. The hypervalent alkanium ion also explains the stronger dependency of the transition state energies for the proton exchange than for the hydride abstraction reaction. Propane is, perhaps with the exception of ethane, unique in the sense that the reaction rates for both reactions are within the same order of magnitude and are both easily observable.

Propane is also the smallest alkane with two different hydrogen atoms, one on the methylene group (2-H) and one on the methyl groups (1-H). Despite the overall very exothermic reaction ($\Delta E_R = 312$ kJ mol^{-1}) a remarkable selectivity of $k_1/k_2 = 0.123$ is observed. Theoretical calculations pro-

vide an explanation. Even though both (1- and 2-H) barriers are well below the energy of the reactants and only different by 6 kJ mol^{-1}, the remarkable selectivity is explained by the ergodic behaviour of the long-lived reactant complex $[C_3H_8\cdots H_2OOH]^+$ (**13**). The more accurate treatment using RRKM theory gave very satisfactory descriptions of the experimental observations.

In addition to the hydride abstraction mechanism (Reaction (1)) an alternative route for formation of R^+ seems likely for larger alkanes. It involves the proton transfer from H_2OOH^+ to the alkane and H_2 elimination from the transient hypervalent alkanium ion RH_2^+ (Reaction (5)). Butane and isobutane represent borderline cases since they are the smallest alkanes with proton affinities above that of HOOH. The access to the proton transfer initiated mechanism could explain the observed great rate enhancement for the reaction of H_2OOH^+ with propane and isobutane, respectively.

Supporting information

Structures, energies, and frequencies of all stationary points of the potential energy surface can be found in the supporting information.

Acknowledgements

The authors express their gratitude to The Norwegian Research Council (NFR) for post-doctoral fellowship to C.A., and to the Program for Supercomputing (NOTUR) for a generous grant of computing time (Grant no. NN2386K).

Appendix A. Supplementary data

Supplementary data associated with this article can be found, in the online version, at doi:10.1016/j.ijms.2006.05.018.

References

[1] H. Arakawa, M. Aresta, J. Armor, M. Barteau, E. Beckman, A. Bell, J. Bercaw, C. Creutz, D.A. Dixon, D. Dixon, K. Domen, D. DuBois, J. Eckert, E. Fujita, D. Gibson, W. Goddard, D. Goodman, J. Keller, G. Kubas, H. Kung, J. Lyons, L. Manzer, T. Marks, K. Morokuma, K. Nicholas, R. Periana, L. Que, J. Rostrup-Nielson, W. Sachtler, L. Schmidt, A. Sen, G. Somorjai, P. Stair, B. Stults, W. Tumas, Chem. Rev. 101 (2001) 953.
[2] J.A. Labinger, J. Mol. Catal. A: Chem. 220 (2004) 27.
[3] M. Lersch, M. Tilset, Chem. Rev. (Washington, DC, United States) 105 (2005) 2471.
[4] A.M.L. Oiestad, A.C. Petersen, V. Bakken, J. Vedde, E. Uggerud, Angew. Chem. Int. Ed. 40 (2001) 1305.
[5] G.A. Olah, T. Keumi, J.C. Lecoq, A.P. Fung, J.A. Olah, J. Org. Chem. 56 (1991) 6148.
[6] G.A. Olah, D.G. Parker, N. Yoneda, Angew. Chem. 90 (1978) 962.
[7] G.A. Olah, N. Yoneda, D.G. Parker, J. Am. Chem. Soc. 99 (1977) 483.
[8] R.D. Bach, M.-D. Su, J. Am. Chem. Soc. 116 (1994) 10103.
[9] C. Adlhart, O. Sekiguchi, E. Uggerud, Chem. Eur. J. 11 (2005) 152.
[10] G.A. Olah, G. Klopman, R.H. Schlosberg, J. Am. Chem. Soc. 91 (1969) 3261.
[11] G.A. Olah, R.H. Schlosberg, J. Am. Chem. Soc. 90 (1968) 2726.
[12] H. Hogeveen, A.F. Bickel, Recl. Trav. Chim. Pays-Bas 88 (1969) 371.
[13] V.L. Tal'rose, A.K. Lyubimova, Dokl. Akad. Nauk. SSSR 86 (1952) 909.
[14] J.H. Futrell, J. Phys. Chem. 65 (1961) 565.
[15] E.T. White, J. Tang, T. Oka, Science 284 (1999) 135.
[16] A. Goeppert, A. Sassi, J. Sommer, P.M. Esteves, C.J.A. Mota, A. Karlsson, P. Ahlberg, J. Am. Chem. Soc. 121 (1999) 10628.
[17] T. Konishi, K. Yoshida, K. Hayashi, in: J.K.T. Koho (Ed.), Processes for Manufacturing Peroxidized Urea, 2003.
[18] N.G. Adams, D. Smith, J.F. Paulson, J. Chem. Phys. 72 (1980) 4951.
[19] Y. Ikezoe, S. Matsuoka, M. Takebe, A. Viggiano, Gas Phase Ion–Molecule Reaction Rate Constants through 1986, Maruzen, Tokyo, 1987.
[20] M.J. Frisch, G.W. Trucks, H.B. Schlegel, G.E. Scuseria, M.A. Robb, J.R. Cheeseman, J.A. Montgomery, T. Vreven, K.N. Kudin, J.C. Burant, J.M. Millam, S.S. Iyengar, J. Tomasi, V. Barone, B. Mennucci, M. Cossi, G. Scalmani, N. Rega, G.A. Petersson, H. Nakatsuji, M. Hada, M. Ehara, K. Toyota, R. Fukuda, J. Hasegawa, M. Ishida, T. Nakajima, Y. Honda, O. Kitao, H. Nakai, M. Klene, X. Li, J.E. Knox, H.P. Hratchian, J.B. Cross, V. Bakken, C. Adamo, J. Jaramillo, R. Gomperts, R.E. Stratmann, O. Yazyev, A.J. Austin, R. Cammi, C. Pomelli, J.W. Ochterski, P.Y. Ayala, K. Morokuma, G.A. Voth, P. Salvador, J.J. Dannenberg, V.G. Zakrzewski, S. Dapprich, A.D. Daniels, M.C. Strain, O. Farkas, D.K. Malick, A.D. Rabuck, K. Raghavachari, J.B. Foresman, J.V. Ortiz, Q. Cui, A.G. Baboul, S. Clifford, J. Cioslowski, B.B. Stefanov, G. Liu, A. Liashenko, P. Piskorz, I. Komaromi, R.L. Martin, D.J. Fox, T. Keith, M.A. Al-Laham, C.Y. Peng, A. Nanayakkara, M. Challacombe, P.M.W. Gill, B. Johnson, W. Chen, M.W. Wong, C. Gonzalez, J.A. Pople, Gaussian 03, Revision C.02, Gaussian, Inc., Wallingford, CT, 2004.
[21] L.A. Curtiss, K. Raghavachari, P.C. Redfern, V. Rassolov, J.A. Pople, J. Chem. Phys. 109 (1998) 7764.
[22] J.K. Laerdahl, E. Uggerud, Org. Biomol. Chem. 1 (2003) 2935.
[23] E.L. Oiestad, J.N. Harvey, E. Uggerud, J. Phys. Chem. A 104 (2000) 8382.
[24] E.L. Oiestad, E. Uggerud, Int. J. Mass Spectrom. 185/186/187 (1999) 231.
[25] J.L. Beauchamp, in: P.B. Armentrout (Ed.), Encyclopedia of Mass Spectrometry, volume 1: Theory and Ion Chemistry, Elsevier, Amsterdam, 2003, p. 843.
[26] C. Adlhart, E. Uggerud, Phys. Chem. Chem. Phys. 9 (2006) 1066.
[27] S.G. Lias, J.E. Bartmess, J.F. Liebman, J.L. Holmes, R.D. Levin, W.G. Mallard, J. Phys. Chem. Ref. Data, Suppl. 17 (1988) 1.
[28] E. Uggerud, Eur. J. Mass Spectrom. 6 (2000) 131.
[29] P.M. Esteves, C.J.A. Mota, A. Ramirez-Solis, R. Hernandez-Lamoneda, J. Am. Chem. Soc. 120 (1998) 3213.
[30] J.O. Hirschfelder, J. Chem. Phys. 6 (1938) 795.
[31] C.E. Dykstra, A.S. Gaylord, W.D. Gwinn, W.C. Swope, H.F. Schaefer, J. Chem. Phys. 68 (1978) 3951.
[32] T. Oka, Phys. Rev. Lett. 45 (1980) 531.
[33] L.I. Yeh, J.M. Price, Y.T. Lee, J. Am. Chem. Soc. 111 (1989) 5597.
[34] P.M. Esteves, A. Ramirez-Solis, C.J.A. Mota, J. Braz. Chem. Soc. 11 (2000) 345.
[35] S.S. Arzumanov, S.I. Reshetnikov, A.G. Stepanov, V.N. Parmon, D. Freude, J. Phys. Chem. B 109 (2005) 19748.
[36] NIST, Standard Reference Database Number 69, 2005, http://webbook.nist.gov/chemistry/.